Electronic Supplementary Material (ESI) for Physical Chemistry Chemical Physics.

Supporting Information

On the use of the Cu^{2+}-iminodiacetic acid complex for double histidine based distance measurements by pulsed ESR

Matthew J. Lawless, Shreya Ghosh, Timothy F. Cunningham†, Amit Shimshi and Sunil Saxena

Department of Chemistry, University of Pittsburgh, 219 Parkman Ave., Pittsburgh, PA 15260

†Current address: Department of Chemistry, Hanover College, 484 Ball Dr., Hanover, IN 47243

Table of Contents

Results

Bis-complex formation inhibited by coordinating ligands

We use CW ESR to determine if the Cu^{2+}-IDA_2 bis-complex is present in solution at the 1:2 Cu^{2+}:IDA ratio. Figure S1 shows the CW spectra of Cu^{2+}:IDA at two different ratios: 1.0:0.5 (solid) and 1.0:2.0 (dotted). At the 1.0:0.5 ratio, there should be no bis-complex formed. As evident in Figure S1, with the addition of the excess IDA, the $g_{||}$ value decreases while the $A_{||}$ increases (shown by shift from dashed grey lines to solid lines). These shifts are consistent with an increase in nitrogen coordination.[1] Therefore, the data suggests that at the 1:2 ratio suggested by Figure 2, there is predominantly Cu^{2+}-IDA_2 bis-complex in solution. In the bis-complex, all four equatorial coordinating ligands are occupied[2] which would inhibit dHis coordination. The mono-complex to bis-complex formation is shown in the inset in Figure S1.

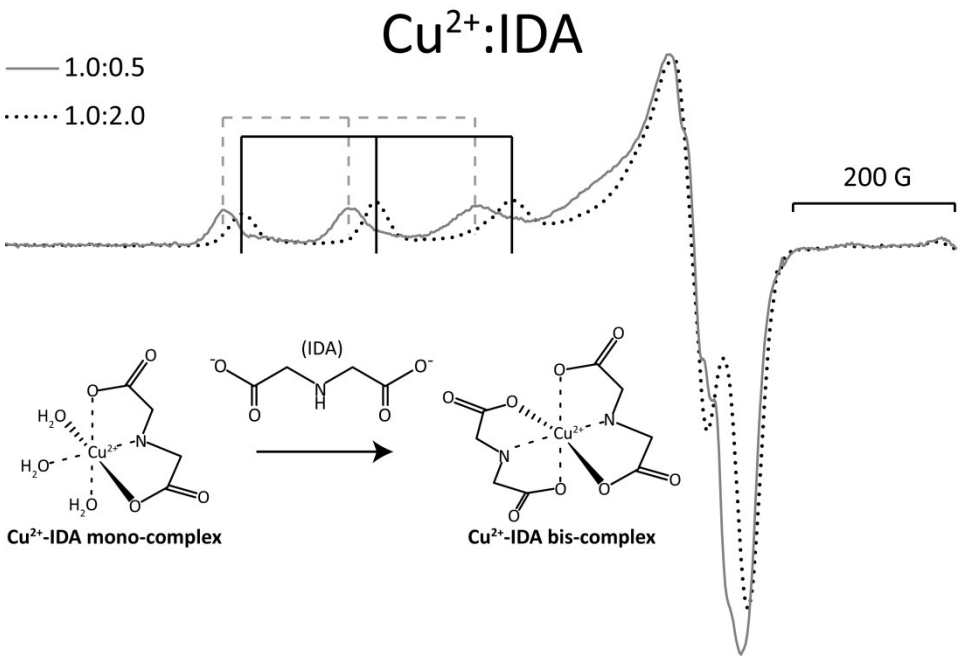

Figure S1: The CW ESR spectra of Cu^{2+}:IDA at two different ratios: 1.0:0.5 (solid) and 1.0:2.0 (dotted). The 1.0:0.5 ratio should consist of entirely of Cu^{2+}-IDA mono-complex. Upon addition of excess IDA, the lineshape shifts. The $g_{||}$ decreases while $A_{||}$ increases as shown by shift from dashed lines to solid lines. This shift is consistent with increased nitrogen coordination. This data suggests that at the 1.0:2.0 ratio of Cu^{2+}:IDA, the bis-complex is predominant in solution. Mono-complex to bis-complex formation shown in inset.

It has been documented that in the presence of a coordinating ligand, the Cu^{2+}-IDA_2 bis-complex is inhibited.[3] Therefore, we use CW ESR in order to detect if the bis-complex formation is inhibited by the presence of the coordinating ligand of the dHis motif: imidazole. Figure S2 shows the CW spectra of Cu^{2+} in the presence of both IDA and imidazole at two different ratios of Cu^{2+}:IDA:Imidazole, 1:1:1 (solid) and 1:2:1 (dotted). As evident from Figure S2, the addition of excess IDA does not alter the lineshape. This data suggests that at the Cu^{2+}:IDA ratio of 1:2 suggested by Figure 2, the bis-complex formation will be inhibited in the presence of imidazole. The imidazole-Cu^{2+}-IDA inhibition of the bis-complex is shown in the inset of Figure S2. Further

supporting these results are ESEEM spectra shown in Figure S3. Figure S3 shows the ESEEM spectra of both Cu^{2+}:IDA and Cu^{2+}:IDA:imidazole (1:2 and 1:2:1 respectively). The ESEEM spectrum of Cu^{2+}:IDA:imidazole (grey line) clearly shows the presence of imidazole coordination as compared to the Cu^{2+}:IDA ESEEM spectrum (black dashed) which is largely featureless.

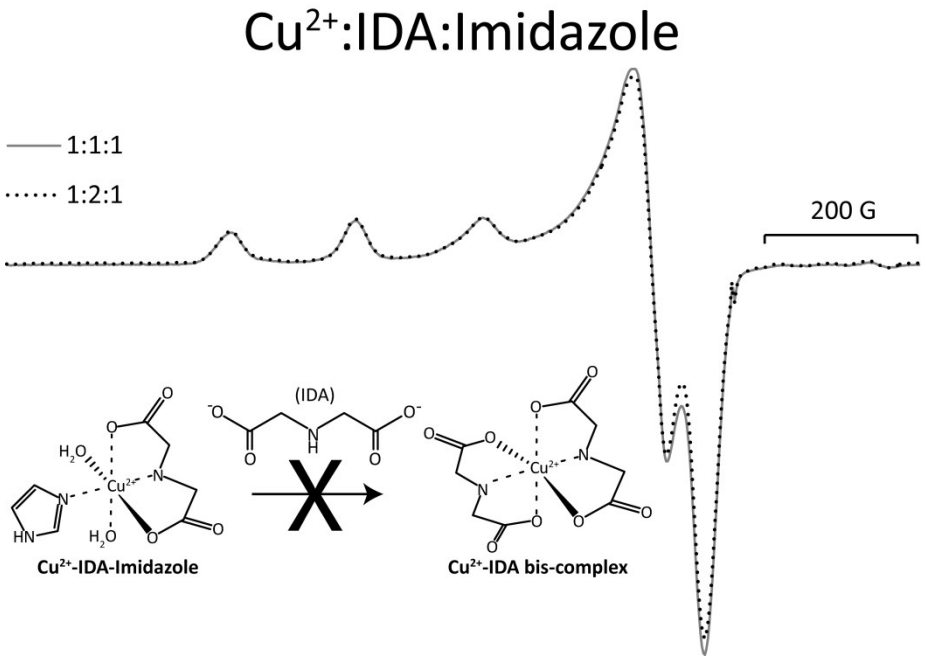

Figure S2: The CW ESR spectra of Cu^{2+} in the presence of both IDA and imidazole at two different ratios of Cu^{2+}:IDA:Imidazole, 1:1:1 (solid) 1:2:1 (dotted). The lineshape does not change upon the addition of excess IDA. This suggests that the imidazole coordinating ligand inhibits the formation of the Cu^{2+}-IDA_2 bis-complex. This inhibition is shown in the inset.

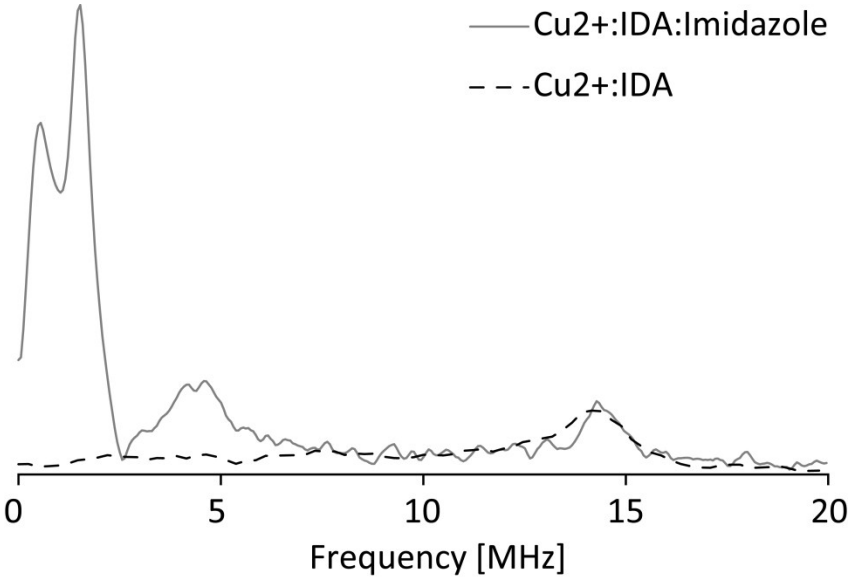

Figure S3: Fourier transformed ESEEM spectra of Cu^{2+}:IDA (black dashed) and Cu^{2+}:IDA:imidazole (grey line) solutions (1:2 and 1:2:1 respectively) in NEM buffer at pH 7.4. Even in the presence of two fold IDA, Cu^{2+} complexes

with the imidazole nitrogen as evident from the features below 2 MHz and at 4 MHz. This further supports that introduction of a coordinating ligand inhibits biscomplex formation.

Taking the data from Figure 2, the pK_d of Cu^{2+}-IDA complexation was calculated to be 5.1 at 80 K as shown in Figure S4. The pK_d of 10.63 was measured under the experimental condition of 293 K[2].Using the enthalpy value for Cu^{2+}-IDA complex formation[4], we can calculate the expected pK_d for Cu^{2+}-IDA at 80 K using the previously published value of 10.63[2]. Using the van't Hoff equation we get a pK_d of 4.3 for Cu^{2+}-IDA at 80 K, which is close to the experimental obtained value of 5.1. Keeping in mind that the literature values were reported at certain ionic strength, the expected and experimental pK_d values differ slightly as our experimental conditions had zero ionic strength. Furthermore, the binding of Cu^{2+}-IDA to imidazole on proteins has been shown to be optimized at pH 7.5[5].

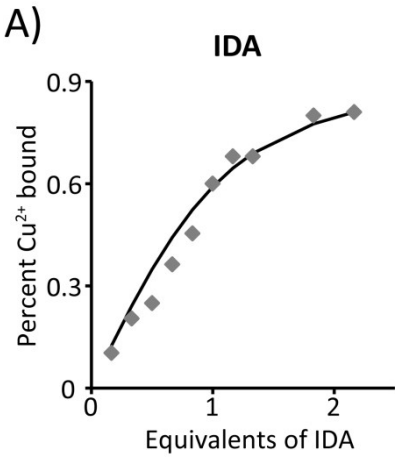

Figure S4: A) Apparent dissociation constant (K_d) fitting of Cu^{2+}:IDA titration resulting in K_d = 70 μM.

Apparent dissociation constants were calculated using the following equation:

$$y = \frac{1}{2}\left(((n+1)[B] + K_d) - \sqrt{((n+1)[B] + K_d)^2 - \left(4n[B]^2\right)}\right) \quad (7)$$

where y is the bound Cu^{2+}, n is the equivalents of Cu^{2+} added, $[B]$ is the concentration of binding site (in this case the concentration of IDA, and K_d is the apparent dissociation constant that was varied until a suitable curve was obtained.

Cu^{2+}-IDA: bound to dHis versus free in solution

The Continuous wave (CW) ESR spectrum lineshape is sensitive to the directly coordinated environment of the bound Cu^{2+}. Figure S3 shows the CW spectrum of Cu^{2+}-IDA with 28H/32H-GB1 (solid) overlaid with the spectrum of Cu^{2+}-IDA alone in solution (dotted). As evident in Figure S5, the spectrum of Cu^{2+}-IDA with 28H/32H-GB1 is a two component lineshape clearly seen in the $g_{||}$ region as indicated by the dashed box. The inset in Figure S5 shows a magnified view of the $g_{||}$ region highlighting both component 1 and component 2, (black lines and grey dashed lines respectively). The Cu^{2+}-IDA spectrum overlays exactly on what we call component 2. Therefore, the data suggests that component 2 is the contribution of unbound Cu^{2+}-IDA in solution.

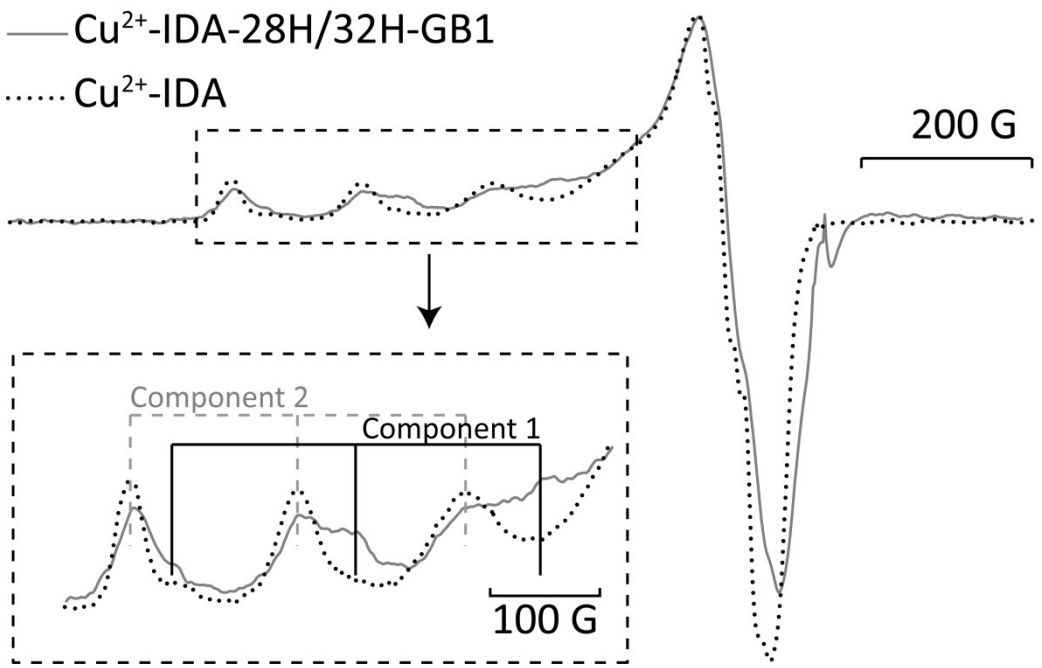

Figure S5: The CW ESR spectrum of Cu^{2+}-IDA in the presence of 28H/32H-GB1 (solid) overlaid with the CW ESR spectrum of unbound Cu^{2+}-IDA in solution (dotted). The spectrum Cu^{2+}-IDA in the presence of 28H/32H-GB1 clearly has two components, as evident in the $g_{||}$ region indicated by dashed box. The inset is a magnified view of the $g_{||}$ region showing component 1 (solid lines) and component 2 (grey dashed lines). Component 2 overlays exactly with the spectrum of unbound Cu^{2+}-IDA in solution. Therefore, the data suggests that the second component is due to free Cu^{2+}-IDA in solution.

dHis loading analyzed by CW spectroscopy

We use CW ESR spectra obtained from Figures 3 and 4 to analyze the percent of dHis sites loaded in the overall sample. The amount of bound Cu^{2+}-IDA per unbound Cu^{2+}-IDA as well as the percent of dHis sites loaded for both α-helix and β-sheet are shown in Figure S6. The doubly integrated intensity of the CW signal is directly proportional to the number of spins present. Through comparison of the doubly integrated intensity to a previously acquired calibration curve, the overall Cu^{2+} concentration is obtained. Furthermore, from our CW simulations from Figures 3 and 4, we derive the percent contributions of the overall signal from both Cu^{2+}-IDA bound to dHis and unbound Cu^{2+}-IDA in solution. The amount of bound Cu^{2+}-IDA per unbound Cu^{2+}-IDA is shown in Figure S6 (solid gray line) for both α-helix and β-sheet. From the overall Cu^{2+} concentration, and from the percentages determined from Figures 3 and 4, we can compare the amount of bound Cu^{2+}-IDA to the known protein concentration to determine the percent of dHis sites loaded. The percent of dHis sites loaded with respect to the amount of equivalents of Cu^{2+}-IDA added for both α-helix and β-sheet is shown in Figure S6 (black dashed line). It is evident that the dHis site located in the β-sheet has a much higher binding efficiency than the dHis site within an α-helix. The titrations from Figures 3 and 4 were converted into Cu^{2+}-IDA bound per dHis site as a function of equivalents of added Cu^{2+}-IDA. The data is shown in Figure S7. This curve was fit to determine the apparent dissociation constants (Kd) using Eq. 7. The K_d for 28H32H-GB1 and 6H8H-GB1 are 1210 μM and 30 μM, respectively indicating a much weaker binding affinity for the α-helical dHis site compared to that of a β-sheet. Full loading of the β-sheet

dHis site is obtained at two equivalents of Cu^{2+}-IDA added. However, as shown in Figure S6, past one equivalent there is a considerable increase in the amount of unbound Cu^{2+}-IDA present which contributes to a decrease in modulation depth in DEER. Since the α-helical dHis site takes far greater than two equivalents to fully load, one equivalent of Cu^{2+} per dHis site was chosen for DEER.

Figure S6: The amount of bound Cu^{2+}-IDA per unbound Cu^{2+}-IDA free in solution with respect to the equivalents of Cu^{2+}-IDA added (solid gray line) for both α-helix (left) and β-sheet (right). It is evident that the β-sheet has much higher

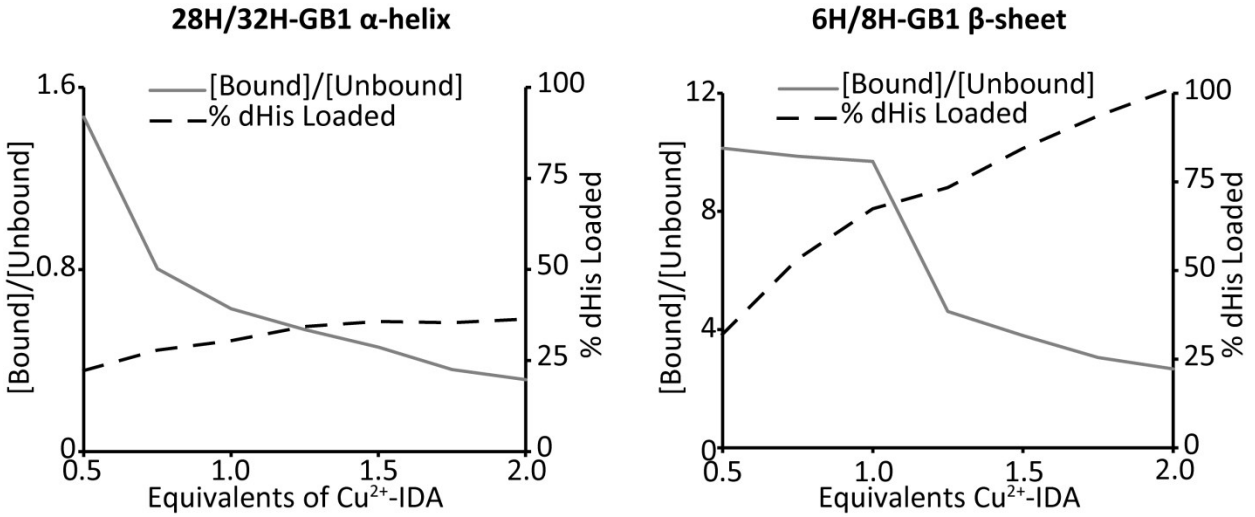

selectivity than the α-helical dHis binding site. Also shown is the percent of dHis loaded (dashed black line). The β-sheet loads far quicker than the α-helix and is capable of full loading.

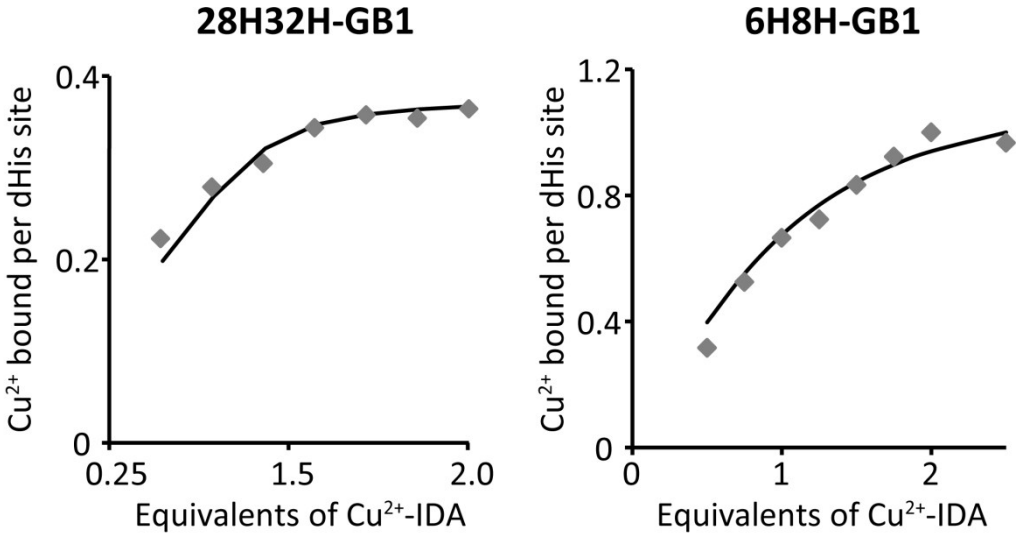

Figure S7: Apparent dissociation constant fits of titration curves of 28H32H-GB1 (left) and 6H8H-GB1 (right) with respect to equivalents of Cu^{2+}-IDA added.

ESEEM titrations

ESEEM signals were collected for both 28H/32H-GB1 and 6H/8H-GB1 at varying equivalents of Cu^{2+}-IDA. Figure S8 shows all ESEEM signals of dHis within an α-helix (left) and β-sheet (right). Data was normalized to point of maximum intensity.

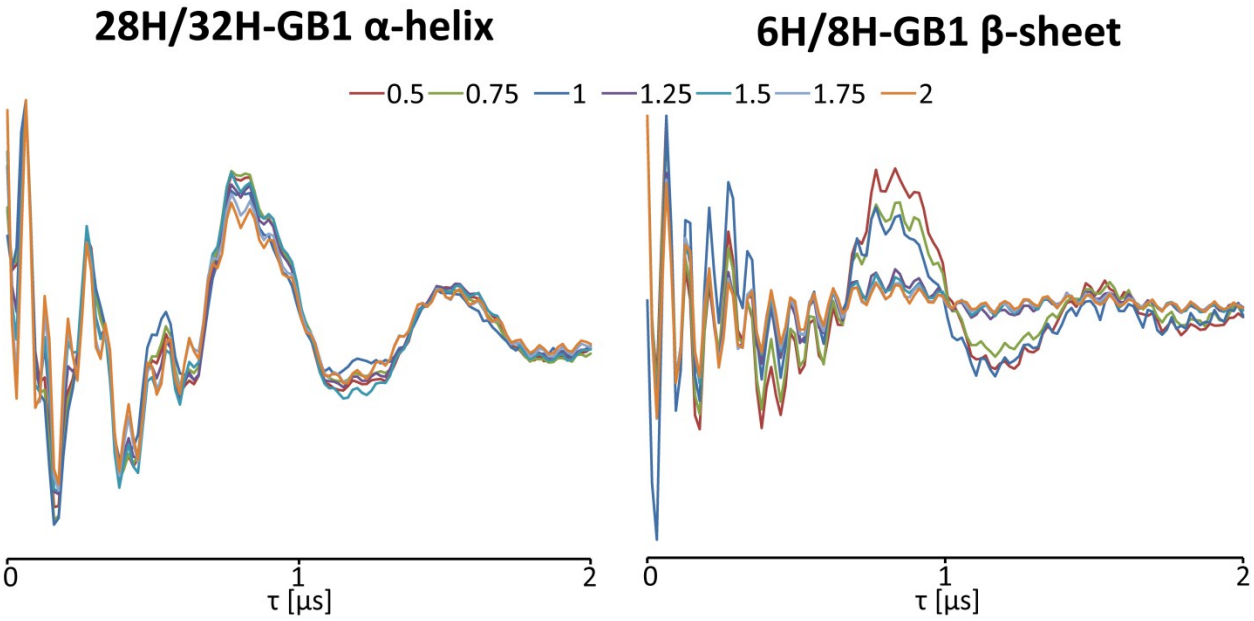

Figure S8: ESEEM signal on dHis site located within an α-helix (left) and β-sheet (right) at seven different equivalents of Cu^{2+}-IDA. Data was normalized to the point of maximum intensity.

DEER Spectroscopy

Figure S9 shows the raw DEER data. Figure S10 shows a comparison of DEER data collected via two differing methods using a Cu^{2+}:IDA ratio of 1:2: pre-incubation of protein with IDA prior to addition of Cu^{2+}, and addition of Cu^{2+}-IDA as a stock solution. As shown in Figure S10, the addition of Cu^{2+}-IDA as a stock solution yields a lower modulation depth.

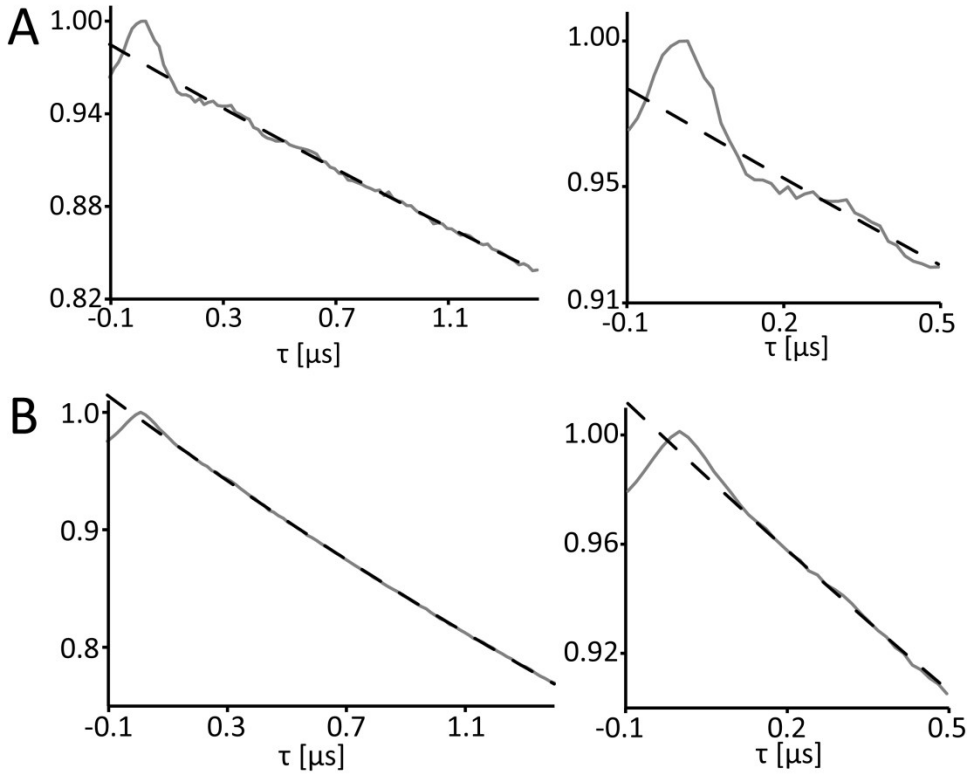

Figure S9: Left) Raw time domain DEER data for 6H/8H/28H/32H-GB1 at two different Cu^{2+}:IDA:dHis ratios: A) 1:2:1, B) 1:1:1. Right) Magnified raw time domain DEER signal to clearly see dipolar modulations for both samples.

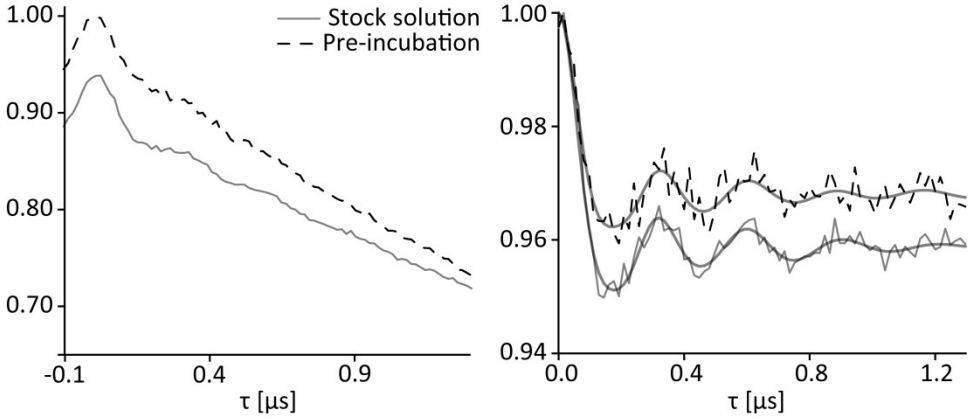

Figure S10: Left) Raw DEER time domain data for 6H/8H/28H/32H-GB1 prepared in two different methods: addition of Cu^{2+}-IDA (1:2 ratio) stock solution (dashed black line) and prepared via pre-incubation of protein with IDA followed by addition of Cu^{2+} (grey solid). Data was offset for clarity. Right) Background subtracted DEER time domain data illustrating the improvement of modulation depth by pre-incubation of protein with IDA followed by the addition of Cu^{2+} (~3.2% to ~4.0%).

CW of dHis with two equivalents of IDA

CW spectroscopy affirms the lack of bis-complex in the tetramutant sample as evident in Figure S11.

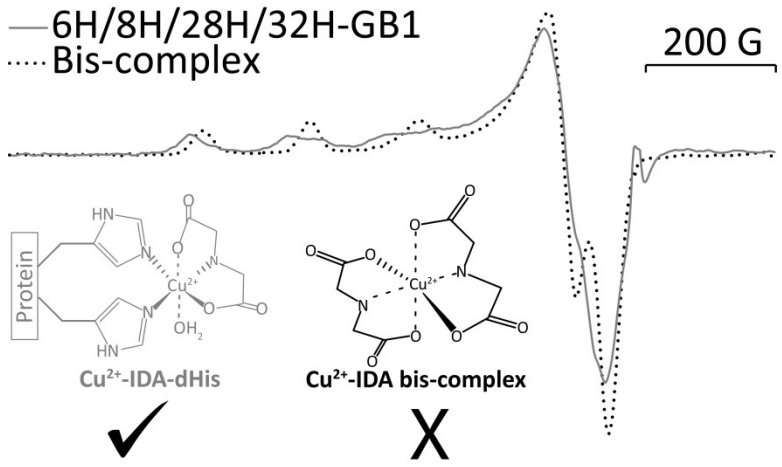

Figure S11: The CW ESR spectrum of 6H/8H/28H/32H-GB1 (gray solid lines) overlaid with the spectrum of the bis-complex (black dotted lines). It is evident that the bis-complex is not present in solution for the 6H/8H/28H/32H-GB1 sample. Inset shows the favored dHis coordination compared to the bis-complex.

The CW spectra (solid gray lines) for 28H/32H-GB1 and 6H/8H-GB1 using 1 equivalent of Cu^{2+} and 2 equivalents of IDA and their respective simulations (dashed black lines) are shown in Figure S12. To prevent bis-complex formation, IDA was added to the protein prior to the addition of the Cu^{2+}. For both sites, the amount of dHis sites loaded increased compared to the equimolar IDA solution. Note that there is increased super hyperfine features in the $g_{\perp}$ which is indicative of a more homogeneous binding environment. Furthermore, this superhyperfine structure was simulated using parameters of three equatorial coordinated nitrogen. This superhyperfine structure is not evident in Figure 3 most likely due to inconsistent coordination, due to the possibility of IDA-free Cu^{2+} occupying the dHis site.

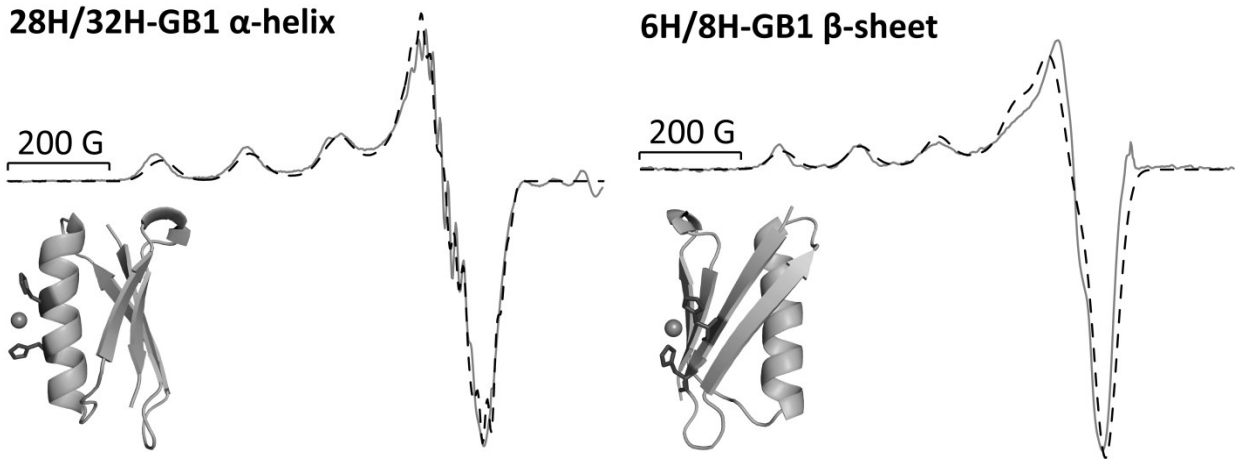

Figure S12: The CW ESR spectra (gray solid lines) and respective simulations (black dashed lines) 28H/32H-GB1 (left) and 6H/8H-GB1 with one equivalent of Cu^{2+} and two equivalents of IDA. Both spectra were fit with two components, the second using parameters consistent with unbound Cu^{2+}-IDA in solution. The percent of dHis loaded increased for both α-helix and β-sheet.

1. J. Peisach and W. E. Blumberg, *Arch. Biochem. Biophys.*, 1974, **195**, 691-708.
2. I. Lukes, I. Smidova, A. Vleck and J. Podlaha, *Chem. Zvesti*, 1982, **38**, 331-339.
3. T. Yip, Y. Nakagawa and J. Porath, *Anal. Biochem.*, 1989, **183**, 159-171.
4. T. S. Roche and R. G. Wilkins, *J. Am. Chem. Soc.*, 1974, **96**, 5082-5086.
5. W. Chen, C. Wu and C. Liu, *J. Colloid Interface Sci.*, 1996, **180**, 135-143.